EurJIC
European Journal of Inorganic Chemistry

Research Article
doi.org/10.1002/ejic.202100965

Chemistry Europe
European Chemical Societies Publishing

www.eurjic.org

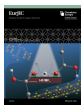

Syntheses and Structures of Protonated Acetylenedicarboxylic Acid

Christoph Jessen[a] and Andreas J. Kornath*[a]

Acetylenedicarboxylic acid ($C_4H_2O_4$) was protonated in the binary superacidic systems HF/MF_5 (M = As, Sb). Depending on the stoichiometric ratio of Lewis acid and acetylenedicarboxylic acid mono- and diprotonated acetylenedicarboxylic acid was obtained. The salts of diprotonated acetylenedicarboxylic acid were characterized by vibrational spectroscopy and in case of $[C_4H_4O_4][SbF_6]_2$ by a single-crystal X-ray structure analysis. The salt crystallizes in the monoclinic space group $C2/c$ with four formula units per unit cell. Furthermore, salts of monoprotonated acetylenedicarboxylic acid were synthesized and characterized by single-crystal X-ray structure analysis. The salts $[C_4H_3O_4][AsF_6]$ and $[C_4H_3O_4][SbF_6]$ crystallize in the monoclinic space group $C2/c$ with four formula units per unit cell. The monoprotonation is better described as a twofold hemiprotonation of acetylenedicarboxylic acid. The experimental results are discussed together with quantum chemical calculations.

Introduction

The acetylenedicarboxylic moiety is a widely applied structure motif in synthetic chemistry. It is commonly used as a dienophile and dipolarophile in cycloaddition reactions, or as Michael acceptor.[1] The acetylenedicarboxylate anion is deployed as ligand for coordination polymers or as building block for metal-organic frameworks (MOFs).[2] Its simplest form - acetylenedicarboxylic acid – was first described by *Bandrowski* in 1877. Since then, the acidic compound (pK_{a1} = 1.75; pK_{a2} = 4.40) and its corresponding anions have been thoroughly characterized. However, to the best of our knowledge the basicity of acetylenedicarboxylic acid has not been reported yet. This prompted us to investigate the behavior of acetylenedicarboxylic acid in superacid media.

Results and Discussion

Syntheses

Acetylenedicarboxylic acid was reacted in the binary superacidic systems XF/MF_5 (X = H, D; M = As, Sb) as shown in equation (1) and equation (2). Both reactions were performed in a two-step synthesis. First, the superacidic system (HF/AsF_5 or HF/SbF_5) was formed by homogenization of the Lewis acid with an excess of anhydrous hydrogen fluoride at −30 °C. After freezing the superacidic system at −196 °C, acetylenedicarboxylic acid was added under inert gas atmosphere. Then the mixture was warmed to −30 °C, where the protonation reaction took place. After the removal of excess aHF at −78 °C *in vacuo* the yellowish salts $[C_4H_4O_4][AsF_6]_2$ (**1**), $[C_4H_4O_4][SbF_6]_2$ (**2**) and the colorless salts $[C_4H_3O_4][AsF_6]$ (**3**), $[C_4H_3O_4][SbF_6]$ (**4**) were obtained. The salts of the diprotonated acetylenedicarboxylic acid (**1**) and (**2**) are stable up −10 °C, while the salts of the twofold hemiprotonated acetylenedicarboxylic acid (**3**) and (**4**) are stable up to 15 °C.

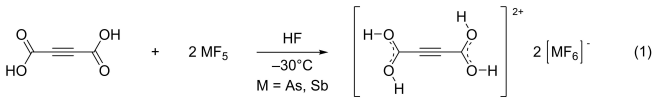

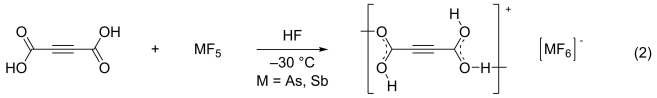

The corresponding deuterated salts $[C_4D_4O_4][AsF_6]_2$ (**5**) and $[C_4D_4O_4][SbF_6]_2$ (**6**) are obtained by changing the superacidic system from HF/MF_5 to DF/MF_5 (M = As, Sb). Due to large excess of aDF (100:1), a deuteration of approximately 98% was achieved.

Crystal Structure of $[C_4H_4O_4][SbF_6]_2$

The salt $[C_4H_4O_4][SbF_6]_2$ (**2**) crystallizes in the monoclinic space group $C2/c$ with four formula units per unit cell. The formula unit is illustrated in Figure 1 and a summary of the geometric parameters is listed in Table 1. In the crystal packing of the starting material, acetylenedicarboxylic acid forms linear chains which are connected by disordered hydrogen bonds. Therefore, the C–O distances are equally long and in the range between regular C–O and C=O bond lengths.[3] Even though diprotonation breaks the $C_4H_2O_4$ chains apart, only small changes in its geometrical parameters are observed when $C_4H_2O_4$ is compared to (**2**). Due to the diprotonation an elongation of the C=O

[a] C. Jessen, Prof. Dr. A. J. Kornath
Department Chemie, Ludwig-Maximilians-Universität München
Butenandtstr. 5–13(D), 81377 München, Germany
E-mail: andreas.kornath@cup.uni-muenchen.de

Supporting information for this article is available on the WWW under https://doi.org/10.1002/ejic.202100965

Research Article
doi.org/10.1002/ejic.202100965

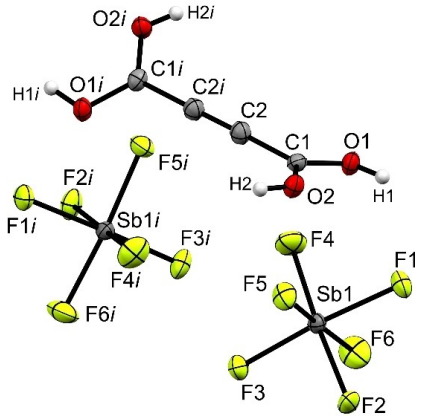

Figure 1. Formula unit of (**2**) (50% probability displacement ellipsoids). Symmetry code: $i = 1-x, y, 0.5-z$.

Table 1. Selected bond lengths and angles of acetylenedicarboxylic acid, $[C_4H_4O_4][SbF_6]_2$ (**2**) and $[C_4H_3O_4][SbF_6]$ (**4**).

Bond lengths [Å]	$C_4H_2O_4$[5]	$[C_4H_4O_4][SbF_6]_2$	$[C_4H_3O_4][SbF_6]$
C1–C2 (C–C)	1.454(1)	1.442(4)	1.446(2)
C2–C2*i* (C≡C)	1.188(1)	1.180(5)	1.188(3)
C1–O1	1.262(1)	1.261(3)	1.282(2)
C1–O2	1.245(1)	1.264(3)	1.237(2)
Bond angles [°]			
O1–C1–O2	126.0(1)	121.2(2)	123.1(1)
O1–C1–C2	116.8(1)	116.0(2)	116.2(1)
O2–C1–C2	117.2(1)	122.8(2)	120.7(1)
C1–C2–C2*i*	177.7(1)	178.9(4)	172.9(1)
Angle of torsion [°]			
O1–C1–C2–C2*i*		142(10)	−165(1)
O2–C1–C2–C2*i*		−39(10)	14(1)
C1–C2–C2*i*–C1*i*		−146(13)	42(2)
Donor-acceptor distances [Å]			
O1–H1···F2*ii*		2.544(3)	
O2–H2···F1		2.537(2)	
O2–H2···O2*iii*			2.442(2)
O1–H1···F1			2.578 (2)

bonds of 0.019 Å is observed, which leads to bond lengths of 1.261(3) (C1–O1) and 1.264(3) Å (C1–O2) in (**2**). The positive charges are stabilized within the carboxy groups. This is also observed in the structurally similar tetrahydroxydicarbenium cation $[(HO)_2CC(OH)_2]^{2+}$ with C–O bond lengths of 1.257(2) Å and 1.259(3) Å.[4] On the contrary, the C–C and C≡C bonds are not significantly affected by the diprotonation. The $[C_4H_4O_4]^{2+}$ cation does not show a planar structure with the protonated carboxy groups being twisted with respect to each other by 41.10°.

The Sb–F bond lengths of the $[SbF_6]^-$ anion range from 1.848(2) to 1.917(2) Å. The values are typical for slightly distorted $[SbF_6]^-$ anions.[6–8] The distortion from the octahedral structure is caused by hydrogen bonds with the cation, which leads to an elongation of the Sb-F1 and Sb-F2 bonds.

Vibrational Spectra of $[C_4H_4O_4][SbF_6]_2$

Selected infrared and Raman spectra of $[C_4H_4O_4][SbF_6]_2$ (**2**), $[C_4D_4O_4][SbF_6]_2$ (**6**) and the starting materials $C_4H_2O_4$ and $C_4D_2O_4$ are shown in Figure 2. Table 2 summarizes selected experimental vibrational frequencies together with calculated frequencies of the $[C_4X_4O_4 \cdot 4HF]^{2+}$ cation (X = H, D). The vibrational spectra of all synthesized salts of diprotonated acetylenedicarboxylic acid and their respective D-isotopomers are illustrated in the Supporting Information (Figure S2). According to the crystal structure, the dication possesses C_2 symmetry with 30 fundamental vibrations. All of them are expected to be IR and Raman active. The assignment is based on an analysis of the Cartesian displacement vectors of the calculated vibrational modes and a comparison with the vibrations described in the literature for $C_4H_2O_4$.[9]

The O–H stretching vibrations of (**2**) are not observed in the Raman spectrum due to the poor polarizability of the OH group. However, in the vibrational spectra of $[C_4D_4O_4][SbF_6]_2$ (**6**) the O–D stretching vibrations can be observed between 2126 cm^{-1} and 2016 cm^{-1} (Ra), and as a broad band between 2015 cm^{-1} and 2083 cm^{-1} (IR). The characteristic C≡C stretching mode is observed at 2301 cm^{-1} (**1**) and 2290 cm^{-1} (**2**), respectively with blue-shifts of 60 cm^{-1} (**1**) and 49 cm^{-1} (**2**) compared to the neutral compound.[9] The diprotonation of acetylenedicarboxylic acid is confirmed by the shifts of the CO stretching modes. The C=O stretching vibrations of $C_4H_2O_4$ at 1697 cm^{-1} and 1659 cm^{-1} are red-shifted in the diprotonated species (1644 cm^{-1} (**1**), 1645 cm^{-1} (**2**) (Ra) and 1634 cm^{-1} (**1**), 1632 cm^{-1} (**2**) (IR)).

The intense Raman lines at 1533 cm^{-1} (**1**) and 1529 cm^{-1} (**2**), respectively can be assigned to the other C–O stretching vibrations. Compared to the neutral compound, these ν(C–O)

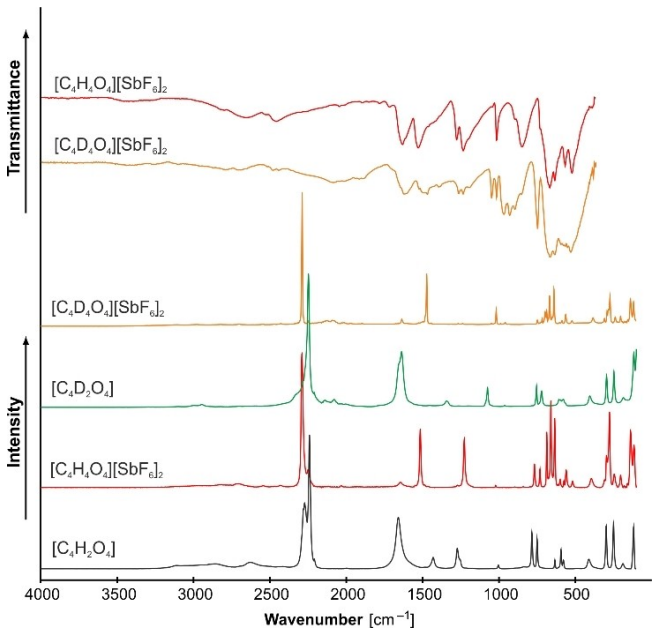

Figure 2. Low-temperature Raman and IR spectra of $[C_4X_4O_4][SbF_6]_2$ (X=H, D) (**2**, **6**), $C_4H_2O_4$ and $C_4D_2O_4$.

Research Article
doi.org/10.1002/ejic.202100965

Table 2. Selected experimental vibrational frequencies [cm^{-1}] of $[C_4X_4O_4][SbF_6]_2$ (X = H, D) and calculated vibrational frequencies [cm^{-1}] of $[C_4X_4O_4 \cdot 4HF]^{2+}$.

$[C_4H_4O_4][SbF_6]_2$ (**2**) exp.[a] IR	Raman	$[C_4D_4O_4][SbF_6]_2$ (**6**) exp.[a] IR	Raman	$[C_4H_4O_4 \cdot 4\ HF]^{2+}$ calc.[b,c] IR/Raman	$[C_4D_4O_4 \cdot 4\ HF]^{2+}$ calc.[b,c] IR/Raman	Assignment[d]
2299 vw	2290 (100)		2290 (100)	2297 (0/517)	2301 (100/488)	ν(C≡C)
1632 m	1645 (4)	1626 m	1633 (6)	1654 (238/7)	1640 (570/4)	ν_s(CO)
	1592 (1)	1605 m	1604 (3)	1654 (594/4)	1639 (277/7)	ν_{as}(CO)
1529 m	1549 (2)	1518 m	1528 (3)	1521 (986/2)	1487 (996/2)	ν_{as}(CO)
	1516 (44)	1475 m	1478 (35)	1503 (78/69)	1462 (18/95)	ν_s(CO)
1277 m	1273 (2)	1016 w	1018 (12)	1247 (320/0)	1000 (59/10)	δ(CO*X*)
1234 m		968 m	989 (2)	1234 (287/1)	946 (142/0)	δ(CO*X*)
	1227 (36)	949 m	959 (3)	1228 (133/29)	929 (11/3)	δ(CO*X*)
	1227 (36)	930 m	936 (2)	1228 (133/29)	910 (180/1)	δ(CO*X*)

[a] Abbreviations for IR intensities: vs = very strong, s = strong, m = medium, w = weak. [b] Calculated on the M06/aug-cc-pVTZ level of theory. Scaling factor: 0.965. [c] IR intensities in km/mol; Raman intensities in Å^4/u. [d] X = H, D.

vibrations are blue-shifted by 110 cm^{-1} (**1**) and 90 cm^{-1} (**2**), respectively. Furthermore, four δ(COH) vibrations are observed between 1277 cm^{-1} (IR, (**2**)) and 1227 cm^{-1} (Ra, (**2**)). As expected, the corresponding δ(COD) vibrations are red-shifted and are observed between 1018 cm^{-1} (Ra, (**6**)) and 930 cm^{-1} (IR, (**6**)). In both compounds, more than the expected vibrations for anions with ideal octahedral symmetry are detected. This indicates a distortion of the $[AsF_6]^-$ and $[SbF_6]^-$ anions which is in accordance with the data from the crystal structure.

Crystal Structure of Monoprotonated Acetylenedicarboxylic Acid $[C_4H_3O_4][MF_6]$ (M=As, Sb)

The salts $[C_4H_3O_4][MF_6]$ (M = As, Sb) crystallize in the monoclinic space group *C*2/*c* with four formula units per unit cell. The crystal structures of (**3**) and (**4**) are isomorphous. Since the geometric parameters of the cation in the two crystal structures do not differ significantly, only the crystal structure of $[C_4H_3O_4][SbF_6]$ (**4**) is discussed in the following part. The formula unit is illustrated in Figure 3 and the selected geometric parameters are listed in Table 1.

The formula unit of the $[AsF_6]^-$ salt (**3**) is depicted in Figure S1 and the geometric parameters of (**3**) and (**4**) are compared in Table S1 in the Supporting Information. On the one hand, the bond lengths of the carbon backbone of (**4**) are not affected by monoprotonation and are comparable to the starting material and $[C_4H_4O_4][SbF_6]_2$ (**2**). On the other hand, the bond lengths in the carboxy group change significantly. The C–O bond lengths of 1.282(2) Å (C1–O1) and 1.237(2) Å (C1–O2) differ by 0.045 Å. Therefore, there is a significant difference between the C–O bond lengths in **3** and **4** in contrast to the diprotonated species **2**, which shows no difference within the estimated standard deviations. This indicates that the positive charge is not equally distributed within the carboxy group as it is in $[C_4H_4O_4][SbF_6]_2$ (**2**). The bond angles in the $[C_4H_3O_4]^+$ cation are between the bond angles of the neutral compound and (**2**). The C1-C2-C2*i* bond angle with 172.9(1)° is surprisingly small for an *sp*-hybridized carbon atom, which results in a bent structure of the carbon scaffold. However, similar and even smaller angles along the carbon chain are well known for the acetylenedicarboxyl moiety.[5] In the $[SbF_6]^-$ anion the Sb–F bond lengths range from 1.851(2) to 1.891(1) Å, which are typical values for slightly distorted $[SbF_6]^-$ anions.[6–8] The distortion from the octahedral structure is due to hydrogen bonding towards the cation.

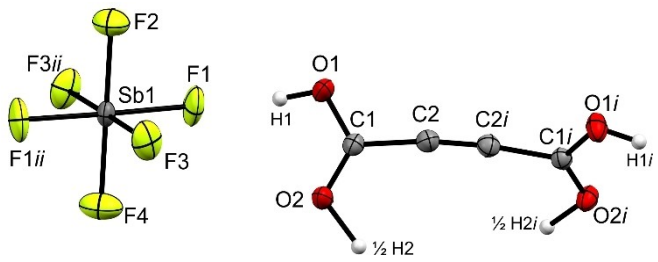

Figure 3. Formula unit of **4** (50% probability displacement ellipsoids). Symmetry codes: *i* = −*x*, *y*, −0.5−*z*; *ii* = 1−*x*, *y*, 1.5−*z*.

The cations in the crystal structure of (**4**) consist of hemiprotonated polycationic chains instead of the monoprotonated species $[C_4H_3O_4][MF_6]$. Therefore, the formally monoprotonated acetylenedicarboxylic acid is better described as twofold hemiprotonated acetylenedicarboxylic acid. A similar structure of polycationic chains with twofold hemiprotonated molecules is observed in monoprotonated *p*-benzoquinone and fumaric acid.[10,11] When formally monoprotonated acetylenedicarboxylic acid (**4**) is compared to monoprotonated oxalic acid, there is an interesting difference in the crystal packing. Oxalic acid shows a clear monoprotonation in its crystal structure, even though it also builds cationic chains via hydrogen bonds (Figure 4). A comparison to the C–O bond lengths in monoprotonated oxalic acid indicates that there is a significant difference between the monoprotonation and the twofold hemiprotonation. However, it should be noted, that the hemiprotonation could indicate an alternating situation between a protonation in one direction or the other. Therefore, the C–O bond lengths in (**4**), involved in the O···H···O hydrogen bonds are expected to be between the corresponding C–O bond lengths of monoprotonated oxalic acid. Indeed, this is observed and shown in Figure 4.

Figure 5 shows the difference electron density map of $[C_4H_3O_4][SbF_6]$ (**4**) in the plane of the two bridged carboxyl groups.

Research Article
doi.org/10.1002/ejic.202100965

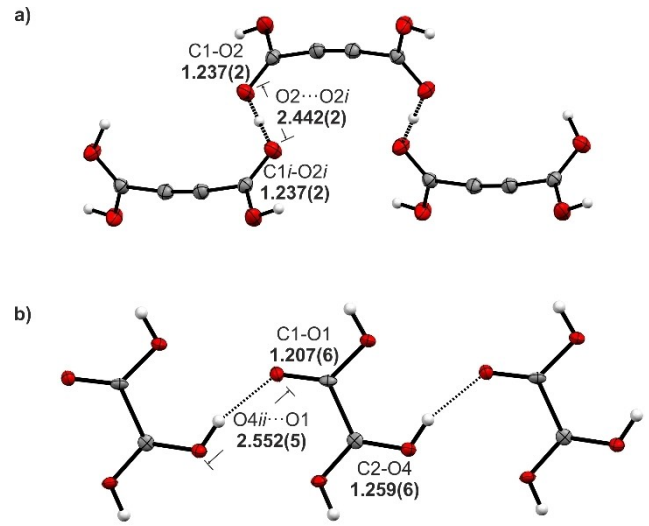

Figure 4. C–O bond lengths and O···O distances in the cationic chains of a) $[C_4H_3O_4][SbF_6]$ (**4**) and b) monoprotonated oxalic acid.[4] Bond lengths are given in Å. Symmetry codes: *i* = 0.5−x, 0.5−y, 1.5−z; *ii* = x, 1.5−y, 0.5+z.

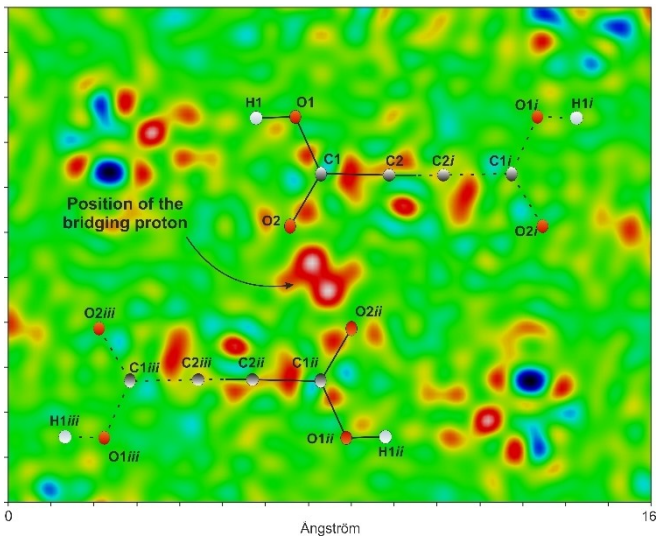

Figure 5. Difference electron density map of the $[C_4H_3O_4]^+$ cation in (**4**) without the bridging proton in the plane of the two bridged carboxyl groups.

Since the exact position of the proton is indeterminate by single-crystal X-Ray analysis, its position is assumed to be between O2 and O2*i*. For crystallographic site symmetry, the structure was successfully refined with the proton located on the inversion center. As the difference electron density map suggests, a twofold disorder with a 50% proton occupation might be present in the crystal structure. Nevertheless, a strong hydrogen bond O2···H···O2*i* with a very short donor-acceptor distance of 2.442(2) Å is present in the crystal structure. The donor-acceptor distance is considerably shorter than the sum of the Van der Waals radii (3.00 Å).[12] Similarly short O···(H)···O distances are observed in the $(H_5O_2^+)$-cation.[13,14] Other comparable hydrogen bonds are described in the literature and are referred to as short, strong, low-barrier (SSLB) hydrogen bonds.[15,16]

Quantum chemical calculations

Quantum chemical calculations were performed on the M06/aug-cc-pVTZ level of theory with the Gaussian program package. To simulate the strong hydrogen bonds, observed in the crystal structure, four hydrogen fluoride molecules were added to the gas phase structure of the $[C_4H_4O_4]^{2+}$ cation.[4,17] Figure 6 shows the experimental and calculated structure of the $[C_4H_4O_4]^{2+}$ moiety in the $[C_4H_4O_4 \cdot 4HF]^{2+}$ cation with bond lengths and angles.

The calculated gas phase structure is in good agreement with the structure observed in the crystal structure. Also the experimental vibrational frequencies are better represented by the calculated HF solvated cation than by the naked $[C_4H_4O_4]^{2+}$ cation. The calculation of the gas phase structure of the monoprotonated cation is more complex. Due to the twofold hemiprotonation, the $[C_4H_3O_4]^+$ cation possesses C_2 symmetry in the crystal structure of (**3**) and (**4**). However, the gas phase structure of the naked $[C_4H_3O_4]^+$ cation possesses C_1 symmetry and describes the geometrical parameters of the $[C_4H_3O_4]^+$ cation only poorly. To address this issue in the calculation, two HF molecules were added to simulate anion-cation contacts and two formaldehyde molecules were added to simulate the interactions of the cationic chain in the solid state (Figure 7). This approach has already been successfully applied to simulate hydrogen bonding and is in good accordance with the data from the crystal structures (**3**) and (**4**).[11,18]

Comparing the crystal and calculated gas phase structures, it stands out that the carbon scaffold is not changed significantly by the degree of protonation. Therefore, it is interesting to compare the protonated species of this work with anionic species of acetylenedicarboxylic acid from the literature.

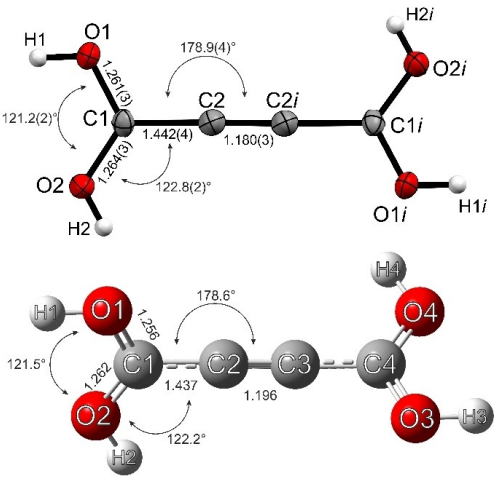

Figure 6. Experimental (top) and calculated (bottom) cationic structures of $[C_4H_4O_4 \cdot 4HF]^{2+}$. The HF molecules are omitted in the depiction of the calculated structure for clarification. Bond lengths are given in Å. Symmetry code: *i* = 1-*x*, *y*, 0.5-*z*.

Research Article
doi.org/10.1002/ejic.202100965

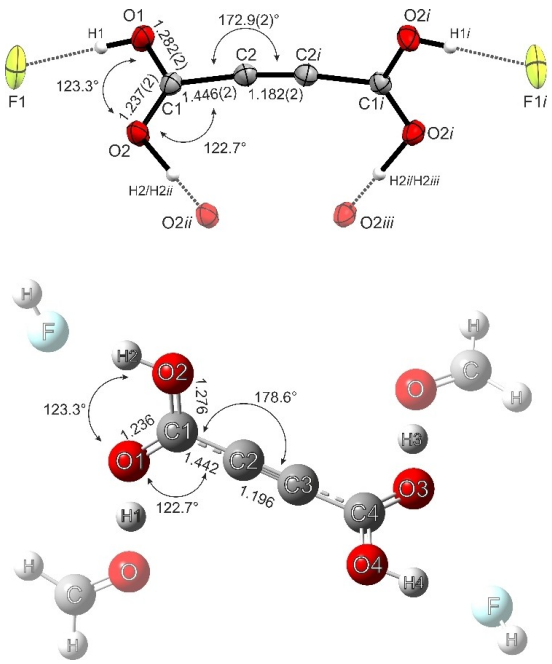

Figure 7. Experimental (top) and calculated (bottom) cationic structures of $[C_4H_4O_4 \cdot 2CH_2O \cdot 2HF]^{2+}$. The intermolecular contacts, HF and formaldehyde molecules, are displayed transparently for clarification. Bond lengths are given in Å. Symmetry code: $i = -x, y, -0.5-z$; $ii = 0.5-x, 0.5-y, -z$; $iii = -0.5+x, 0.5-y, -0.5+z$.

Table 3 summarizes the bond lengths of $[NH_4]_2[C_4O_4]$,[19] $K[C_4HO_4]$,[20] $C_4H_2O_4$,[5] (**2**) and (**4**). The C≡C bond length is not significantly affected by the charge of the acetylenedicarboxylic moiety. However, the C–C single bond length decreases from the dianion to the dication. Interestingly, the C–O bond lengths of the monoanion and monocation differ significantly from the compounds with even charge (−2, 0, +2). Furthermore, the anions in $K[C_4HO_4]$ build infinite chains with very short O···H···O*i* hydrogen bonds (2.446(3) Å).[20] This prompted us to further investigate the hydrogen bonding in twofold hemiprotonated acetylenedicarboxylic acid $[C_4H_3O_4][MF_6]$ (M = As, Sb).

The above-mentioned term of short, strong, low-barrier (SSLB) hydrogen bonds describes a special case of hydrogen bonding, in which the proton is located at a variable position between two similarly acidic acceptor atoms. The main properties of these hydrogen bonds are an unusually short O···O distance of < 2.5 Å and a low or no energy barrier at the symmetric position of the proton between the two acceptor atoms.

Table 3. Summarized bond lengths of selected compounds containing the acetylenedicarboxylic moiety.

Charge	Compound	Bond lengths [Å]		
		C–C	C≡C	C–O
−2	$[NH_4]_2[C_4O_4]$[19]	1.479(3)	1.203(5)	1.252(2)
−1	$K[C_4HO_4]$[20]	1.466(3)	1.191(4)	1.221(3) 1.285(3)
0	$C_4H_2O_4$[5]	1.454(1)	1.188(1)	1.245(1) 1.262(1)
		1.455(1)		1.246(1) 1.259(1)
+1	$[C_4H_3O_4][SbF_6]$	1.446(2)	1.188(3)	1.237(2) 1.282(2)
+2	$[C_4H_4O_4][SbF_6]_2$	1.442(4)	1.180(5)	1.261(3) 1.264(3)

Examples of such hydrogen bonds are observed in O-protonated homodimers of benzophenone, diethyl ether, nitrobenzene or benzaldehyde.[16,21] To investigate if the short hydrogen bonding in (**3**) and (**4**) fits into the concept of SSLB hydrogen bonding, quantum chemical calculations were performed on the B3LYP/aug-cc-pVTZ level of theory. To simulate the O···H···O*i* hydrogen bond in the polycations of (**3**) and (**4**), the calculated structure with two HF and two CH_2O molecules (Figure 7) is not suitable. Therefore, a second approach with a sesquiprotonated dimer was applied as depicted in Figure 8.

The geometry optimization leads to a first-order saddle point on the potential energy surface (TS in Figure 9). At this saddle point, the proton is situated exactly in the middle of the O···H···O trajectory. One single imaginary vibration frequency is calculated for the structure at this saddle point, which refers to the transition state of the proton transfer. The bond lengths and the O···O distance (2.410 Å) in the calculated structure are comparable to the results from the crystal structures (**3**, **4**). Further optimization of the structure with the same O···O distance of 2.410 Å then leads to two equivalent energetic

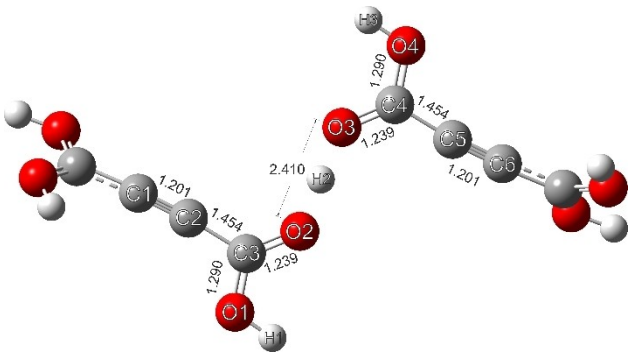

Figure 8. Optimized gas phase structure of the $[(C_4H_3O_4)\cdots H\cdots(C_4H_3O_4)]^{3+}$ cation at the transition state of the proton transfer (first-order saddle point on the potential energy surface). Bond lengths are given in Å.

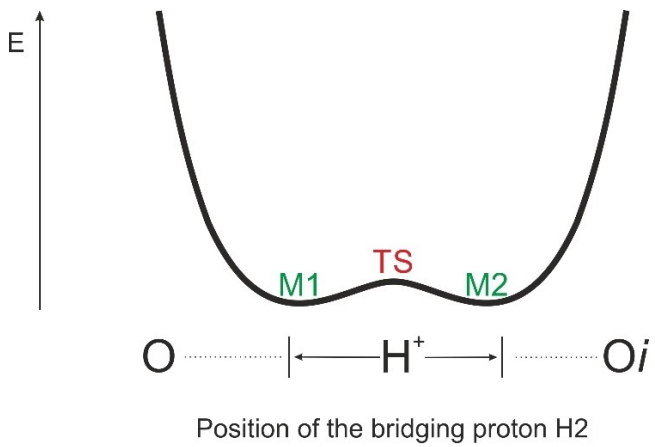

Figure 9. Schematic illustration of the flat bottom energy well typical for short, strong, low-barrier hydrogen bonds.[16,22]

Research Article
doi.org/10.1002/ejic.202100965

minima with the bridging proton being situated slightly outside the central position (M1 and M2 in Figure 9) (Figure S6 Supporting Information). This is consistent with the results of the crystal structure, where the highest electron densities between the O···O*i* atoms are located slightly outside the inversion center (Figure 5). Furthermore, the energy difference between the transition state and the minima is the barrier height of the proton transfer, which is low (1.2 kJ/mol). This indicates an intermediate position of the proton along the O···H···O trajectory, which imposes a small asymmetry since there are two minima that are not located exactly in the middle.

All in all, the experimental and theoretical data for the hemiprotonated hydrogen bond are consistent with the concept of SSLB hydrogen bonding.[16,23] However, this topic has only been reported for proton-bound homodimers so far. Twofold hemiprotonated acetylenedicarboxylic acid shows a polycationic structure which is connected via short, strong hydrogen bonding with indeterminate positioning of the protons.

Conclusion

The reaction of acetylenedicarboxylic acid in the superacidic media HF/AsF_5 and HF/SbF_5 was investigated. The salts of diprotonated $[C_4H_4O_4][MF_6]_2$ (*M*=As, Sb) and monoprotonated $[C_4H_3O_4][MF_6]$ (*M* = As, Sb) acetylenedicarboxylic acid were obtained, depending on the stoichiometric ratio of Lewis acid to starting material. The salts were characterized by low-temperature vibrational spectroscopy and single crystal X-Ray structure analyses. The monoprotonated acetylenedicarboxylic acid is better described as a twofold hemiprotonated species. In the crystal structure short O···H···O hydrogen bonds are present, which build polycationic chains. Furthermore, quantum chemical calculations were performed on the B3LYP/aug-cc-pVTZ level of theory and discussed in context of SSLB hydrogen bonds.

Experimental Section

Caution! Note that any contact with the described compounds should be avoided. Hydrolysis of these salts forms HF which burns skin and causes irreparable damage. Safety precautions should be taken while handling these compounds.

Apparatus and Materials

All reactions were carried out by employing standard Schlenk techniques on a stainless-steel vacuum line. The syntheses of the salts were performed using FEP/PFA-reactors with stainless-steel valves. Before each reaction, the stainless-steel vacuum line and the reactors were dried with fluorine. The obtained compounds were characterized by low temperature IR- and Raman spectroscopy and single crystal X-Ray diffraction analysis. For Raman measurements, a Bruker MultiRam FT-Raman spectrometer with Nd:YAG laser excitation ($\lambda = 1064$ nm) was used. Low temperature IR-spectroscopic investigations were carried out with a Bruker Vertex-80 V FTIR spectrometer using a cooled cell with a single-crystal CsBr plate on which small amounts of the samples were placed.[24] The single crystal X-Ray diffraction studies were performed with an Oxford XCalibur3 diffractometer equipped with a Spellman generator (voltage 50 kV, current 40 mA) and a KappaCCD detector, operating with Mo-K_α radiation ($\lambda = 0.7107$ Å). The measurements were performed at 173 K. The program CrysAlisCCD[25] and for its reduction CrysAlisRED[26] were employed for the data collection. The structures were solved utilizing SHELXS-97[27] and SHELXL-97[28] of the WINGX software package[29] and verified with the software PLATON.[30] The absorption correction was performed using the SCALE3 APSACK multiscan method.[31] Quantum chemical calculations were carried out using the software package Gaussian09.[32]

Syntheses of $[C_4X_4O_4][MF_6]_2$ (*X* = H, D; *M* = As, Sb)

Initially, the binary superacid was formed by condensing the Lewis acid AsF_5 or SbF_5 (1.0 mmol) into a FEP-reactor together with anhydrous hydrogen fluoride (*a*HF) or deuterium fluoride (*a*DF) (1 mL). Both components were then warmed up to −30 °C and homogenized. After freezing the superacidic mixture at −196 °C, acetylenedicarboxylic acid (0.5 mmol) was added to the frozen mixture under nitrogen atmosphere. For the reaction, the mixture was warmed up to −30 °C and homogenized to complete solvation of the starting material. Excess of *a*HF or *a*DF was removed within 14 h at −78 °C. All products were obtained as a yellowish crystalline solid.

Syntheses of $[C_4H_3O_4][MF_6]$ (*M* = As, Sb)

The Lewis acid AsF_5 or SbF_5 (0.5 mmol) was condensed in a FEP reactor vessel together with *a*HF or *a*DF (2 mL) at −196 °C. The superacid was then formed by warming up to −30 °C and homogenization of the components. After freezing the superacidic mixture at −196 °C, acetylenedicarboxylic acid (0.5 mmol) was added to the frozen mixture under nitrogen atmosphere. The reaction mixture was then warmed up to −20 °C and mixed until a clear solution was received. Excess solvent was removed at −78 °C in dynamic vacuum. All products were obtained as a yellowish crystalline solid.

Deposition Numbers 2002493 (for $[C_4H_4O_4][SbF_6]$ (**2**)), 2025068 (for $[C_4H_3O_4][AsF_6]$ (**3**)) and 2025066 (for $[C_4H_3O_4][SbF_6]$ (**4**)) contain the supplementary crystallographic data for this paper. These data are provided free of charge by the joint Cambridge Crystallographic Data Centre and Fachinformationszentrum Karlsruhe Access Structures service www.ccdc.cam.ac.uk/structures.

Acknowledgements

We are grateful to the Department of Chemistry of the Ludwig Maximilian University, Munich, the Deutsche Forschungsgemeinschaft (DFG) and the F-Select GmbH for the support of this work. Open Access funding enabled and organized by Projekt DEAL.

Conflict of Interest

The authors declare no conflict of interest.

Research Article
doi.org/10.1002/ejic.202100965

Data Availability Statement

The data that support the findings of this study are available in the supplementary material of this article.

Keywords: Protonated acetylenedicarboxylic acid · Quantum chemical calculations · Superacidic systems · Vibrational spectroscopy · X-ray diffraction

[1] a) M. Sahoo, *Synlett* **2007**, *2007*, 2142; b) C. Neochoritis, T. Zarganes-Tzitzikas, J. Stephanidou-Stephanatou, *Synthesis* **2014**, *46*, 537.
[2] a) F. Hohn, I. Pantenburg, U. Ruschewitz, *Chem. Eur. J.* **2002**, *8*, 4536; b) I. Stein, U. Ruschewitz, *Z. Naturforsch. B* **2009**, *64*, 1093; c) T. J. M. Ma Ntep, H. Reinsch, B. Moll, E. Hastürk, S. Gökpinar, H. Breitzke, C. Schlüsener, L. Schmolke, G. Buntkowsky, C. Janiak, *Chem. Eur. J.* **2018**, *24*, 14048; d) T. J. Matemb Ma Ntep, H. Reinsch, J. Liang, C. Janiak, *Dalton Trans.* **2019**, *48*, 15849.
[3] A. F. Holleman, N. Wiberg, *Anorganische Chemie*, De Gruyter, Berlin, **2017**.
[4] M. Schickinger, T. Saal, F. Zischka, J. Axhausen, K. Stierstorfer, Y. Morgenstern, A. J. Kornath, *ChemistrySelect* **2018**, *3*, 12396.
[5] A. Delori, I. B. Hutchison, C. L. Bull, N. P. Funnell, A. J. Urquhart, I. D. H. Oswald, *Cryst. Growth Des.* **2018**, *18*, 1425.
[6] R. Minkwitz, C. Hirsch, T. Berends, *Eur. J. Inorg. Chem.* **1999**, *1999*, 2249.
[7] R. Minkwitz, S. Schneider, *Angew. Chem.* **1999**, *111*, 229.
[8] M. Schickinger, C. Jessen, Y. Morgenstern, K. Muggli, F. Zischka, A. Kornath, *Eur. J. Org. Chem.* **2018**, *2018*, 6223.
[9] J. L. Delarbre, L. Maury, L. Bardet, *J. Raman Spectrosc.* **1986**, *17*, 373.
[10] M. Schickinger, M. Siegert, Y. Morgenstern, F. Zischka, K. Stierstorfer, A. Kornath, *Z. Anorg. Allg. Chem.* **2018**, *644*, 1564.
[11] M. C. Bayer, C. Jessen, A. J. Kornath, *Z. Anorg. Allg. Chem.* **2020**.
[12] A. Bondi, *J. Phys. Chem.* **1964**, *68*, 441.
[13] R. Minkwitz, S. Schneider, A. Kornath, *Inorg. Chem.* **1998**, *37*, 4662.
[14] R. Minkwitz, C. Hirsch, *Acta Crystallogr. Sect. C* **1999**, *55*, 703.
[15] a) C. L. Perrin, *Science* **1994**, *266*, 1665; b) L. C. Remer, J. H. Jensen, *J. Phys. Chem. A* **2000**, *104*, 9266; c) C. A. Reed, *Acc. Chem. Res.* **2013**, *46*, 2567.
[16] D. Stasko, S. P. Hoffmann, K.-C. Kim, N. L. P. Fackler, A. S. Larsen, T. Drovetskaya, F. S. Tham, C. A. Reed, C. E. F. Rickard, P. D. W. Boyd et al., *J. Am. Chem. Soc.* **2002**, *124*, 13869.
[17] T. Soltner, N. R. Goetz, A. Kornath, *Eur. J. Inorg. Chem.* **2011**, *2011*, 3076.
[18] M. Schickinger, D. Cibu, F. Zischka, K. Stierstorfer, C. Jessen, A. Kornath, *Chem. Eur. J.* **2018**, *24*, 13355.
[19] I. Stein, C. Näther, U. Ruschewitz, *Solid State Sci.* **2006**, *8*, 353.
[20] I. Leban, L. Golič, J. C. Speakman, *J. Chem. Soc. Perkin Trans. 2* **1973**, 703.
[21] D. Stuart, S. D. Wetmore, M. Gerken, *Angew. Chem. Int. Ed.* **2017**, *56*, 16380.
[22] E. S. Stoyanov, C. A. Reed, *J. Phys. Chem. A* **2006**, *110*, 12992.
[23] S. J. Grabowski, J. M. Ugalde, *Chem. Phys. Lett.* **2010**, *493*, 37.
[24] L. Bayersdorfer, R. Minkwitz, J. Jander, *Z. Anorg. Allg. Chem.* **1972**, *392*, 137.
[25] CrysAlisCCD, *Version 1.171.35.11 (release 16-05-2011 CrysAlis 171.NET)*, Oxford Diffraction Ltd, UK, **2011**.
[26] CrysAlisRED, *Version 1.171.35.11 (release 16-05-2011 CrysAlis 171.NET)*, Oxford Diffraction Ltd, UK, **2011**.
[27] G. M. Sheldrick, *SHELXS-97, Program for Crystal Structure Solution*, University of Göttingen, Germany, **1997**.
[28] G. M. Sheldrick, *SHELXL-97, Program for Crystal Structure Solution*, University of Göttingen, Germany, **1997**.
[29] L. J. Farrugia, *J. Appl. Crystallogr.* **1999**, *32*, 837.
[30] A. L. Spek, *PLATON, A Multipurpose Crystallographic Tool*, Utrecht University, Utrecht, Netherlands, **1999**.
[31] *SCALE3 ABSPACK, An Oxford Diffraction Program*, Oxford Diffraction Ltd, UK, **2005**.
[32] M. J. Frisch, G. W. Trucks, H. B. Schlegel, G. E. Scuseria, M. A. Robb, J. R. Cheeseman, G. Scalmani, V. Barone, B. Mennucci, G. A. Petersson, H. Nakatsuji, M. Caricato, X. Li, H. P. Hratchian, A. F. Izmaylov, J. Bloino, G. Zheng, J. L. Sonnenberg, M. Hada, M. Ehara, K. Toyota, R. Fukuda, J. Hasegawa, M. Ishida, T. Nakajima, Y. Honda, O. Kitao, H. Nakai, T. Vreven, J. A. Montgomery, J. E. Peralta, F. Ogliaro, M. Bearpark, J. J. Heyd, E. Brothers, K. N. Kudin, V. N. Staroverov, R. Kobayashi, J. Normand, K. Raghavachari, A. Rendell, J. C. Burant, S. S. Iyengar, J. Tomasi, M. Cossi, N. Rega, J. M. Millam, M. Klene, J. E. Knox, J. B. Cross, V. Bakken, C. Adamo, J. Jaramillo, R. Gomperts, R. E. Stratmann, O. Yazyev, A. J. Austin, R. Cammi, C. Pomelli, J. W. Ochterski, R. L. Martin, K. Morokuma, V. G. Zakrzewski, G. A. Voth, P. Salvador, J. J. Dannenberg, S. Dapprich, A. D. Daniels, O. Farkas, J. B. Foresman, J. V. Ortiz, J. Cioslowski, D. J. Fox, *Gaussian09, Revision A.02*, Gaussian, Inc, Wallingford CT, **2009**.

Manuscript received: November 9, 2021
Revised manuscript received: December 13, 2021
Accepted manuscript online: December 15, 2021